Available online at www.sciencedirect.com
SCIENCE DIRECT
Tetrahedron
Tetrahedron 62 (2006) 6321–6331

The effect of boronic acid-positioning in an optical glucose-sensing ensemble

Soya Gamsey,[a] Nichol A. Baxter,[a] Zachary Sharrett,[a] David B. Cordes,[a] Marilyn M. Olmstead,[b] Ritchie A. Wessling[a] and Bakthan Singaram[a,*]

[a]*Department of Chemistry and Biochemistry, University of California, Santa Cruz, CA 95064, USA*
[b]*Department of Chemistry, University of California, Davis, CA 95616, USA*

Received 24 February 2006; revised 11 April 2006; accepted 13 April 2006
Available online 12 May 2006

Abstract—The quenching of the anionic dye 8-hydroxypyrene-1,3,6-trisulfonic acid trisodium salt (pyranine) with three different boronic acid-substituted benzyl viologens was determined, and the fluorescence signal modulation obtained upon addition of glucose to the dye/quencher system was also studied. The benzyl viologen that contains boronic acids in the *ortho*-position (*o*-BBV) was found to display unique behavior, which can be rationalized by a charge neutralization mechanism facilitated by an intramolecular interaction between sp^3 boronate and the quaternary nitrogen of the viologen. Potentiometric titration and ^{11}B NMR spectroscopy were used to generate pH profiles for the boronic acids, which provide additional evidence for the proposed mechanism.

1. Introduction

In recent years, much research has been focused on the development of boronic acid-based chemosensors for the detection of glucose.[1] Such sensors are particularly useful to those suffering from diabetes, since accurate monitoring of blood glucose concentrations is essential for the proper management of this disease.[2–5] Boronic acids have proven to be excellent synthetic receptors for glucose due to their ability to reversibly bind 1,2- and 1,3-diols in aqueous media (Scheme 1).[6–10] In many boronic acid-based sensing systems, the saccharide recognition event is monitored using fluorescence spectroscopy.[11] In such systems, the boronic acid receptor is usually directly attached to the fluorophore, and formation of the cyclic boronate ester upon glucose binding results in fluorescence modulation.[12]

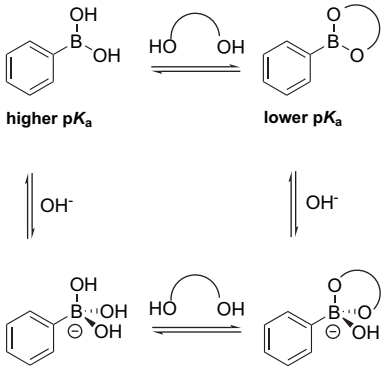

Scheme 1. Equilibria between boronic acids and generic diols.

In contrast to boronic acid-based glucose recognition systems that consist of a single detector molecule, we have developed a two-component sensing system[13] comprising an anionic fluorescent dye (**1**), and a boronic acid-appended cationic viologen (**2**) that dually serves as a fluorescence quencher and a glucose receptor (Scheme 2).[14–17] In the proposed mechanism, the electrostatic association of **1** and **2** results in ground-state complex formation facilitating electron transfer from the dye to the viologen, which leads to a decrease in fluorescence.[18] When glucose is added to the system, formation of two anionic boronate esters effectively neutralizes the dicationic viologen, thus greatly diminishing its quenching efficiency, and an increase in the fluorescence intensity of the dye is observed. Fluorescence modulation is therefore directly correlated with glucose concentration.

In terms of system optimization, the two-component nature of this sensing ensemble allows for a more facile probing of its multivariate space. For example, we have demonstrated that glucose sensing can be carried out using excitation and emission wavelengths across the visible spectrum solely by varying the dye component.[19] Similarly, by modification of the quencher/receptor component, we have investigated the dependence of cationic charge on the sensing

Keywords: Boronic acid; Glucose detection; Fluorescence; pK_a; Viologen; Pyranine; Saccharide sensor.
* Corresponding author. Tel.: +1 831 459 3154; fax: +1 831 459 2935; e-mail: singaram@chemistry.ucsc.edu

0040–4020/$ - see front matter © 2006 Elsevier Ltd. All rights reserved.
doi:10.1016/j.tet.2006.04.047

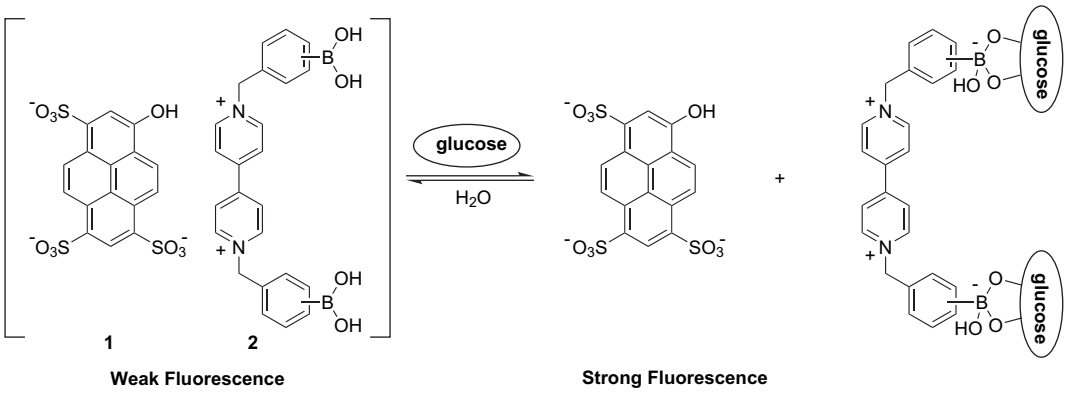

Scheme 2. Proposed mechanism of glucose detection: glucose-induced dissociation of ground-state complex results in fluorescence increase.

mechanism,[20] and also explored the use of phenanthrolinium-based receptors in lieu of viologens (4,4′-bipyridiniums).[21] In the present study, we further probe the system to better understand how positioning of the boronic acid on benzyl viologen affects fluorescence quenching as well as the ability of the quencher/receptor to sense saccharides when used in combination with 8-hydroxypyrene-1,3,6-trisulfonic acid trisodium salt (pyranine, **1**). To help rationalize the observed differences in quenching and glucose sensing, the apparent pK_a values for each of the quencher/receptors were determined by ^{11}B NMR and potentiometric titration. The results of this study provide some insight into the quenching and saccharide sensing mechanisms involved in our two-component system. Such information can be used to aid in the design and optimization of future glucose-sensing systems.

2. Results and discussion

2.1. Description of the system

Three quencher/receptors, *N*,*N*′-4,4′-bis(benzyl-2-boronic acid)-bipyridinium dibromide (*o*-BBV), *N*,*N*′-4,4′-bis(benzyl-3-boronic acid)-bipyridinium dibromide (*m*-BBV), and *N*,*N*′-4,4′-bis(benzyl-4-boronic acid)-bipyridinium dibromide (*p*-BBV), were used to study how positioning of the boronic acid receptor around the benzyl ring affects the system in terms of quenching ability and glucose response (Fig. 1). The non-boronic acid-containing analog, benzyl viologen (BV), was used as a control compound.

The compounds were prepared using a one-step procedure by reacting a twofold excess of bromomethylphenylboronic acid with 4,4′-dipyridyl in DMF. Using acetone, the compounds were precipitated from the reaction mixture in analytically pure form. Recrystallization from water and/or methanol provided single crystals suitable for X-ray analysis. The X-ray crystal structures for *o*-, *m*-, and *p*-BBV are shown in Figure 2.

We anticipated that *o*-BBV would exhibit unique behavior because, in the *ortho*-position, the boronic acid is capable of interacting with the quaternary nitrogen. At pH values above the apparent pK_a of the boronic acid or boronate ester, the boron moiety will exist in its anionic tetrahedral form and a ‘charge neutralization–stabilization mechanism’, previously described by Lakowicz and co-workers for quinolinium benzyl boronic acids[22,23] can occur (Scheme 3). Shinaki and co-workers[16,24–26] have also suggested that an electrostatic interaction is taking place in certain porphyrin-based boronic acids. Both groups agree that the proposed interaction facilitates the formation of boronate ester complexes with saccharides, and have thus integrated this structural motif into glucose sensor designs. The present study provides a systematic investigation in order to verify the

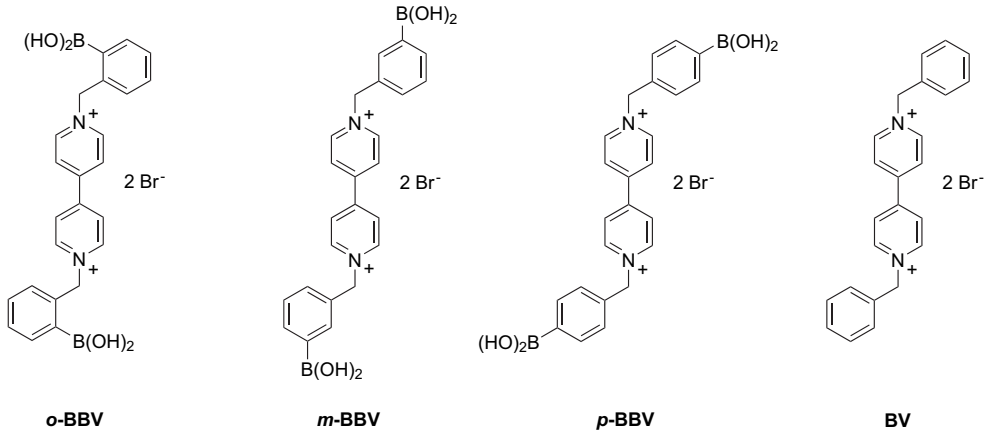

Figure 1. Structures of boronic acid-substituted benzyl viologens, *o*-BBV, *m*-BBV, and *p*-BBV, and their non-boronic acid counterpart, BV.

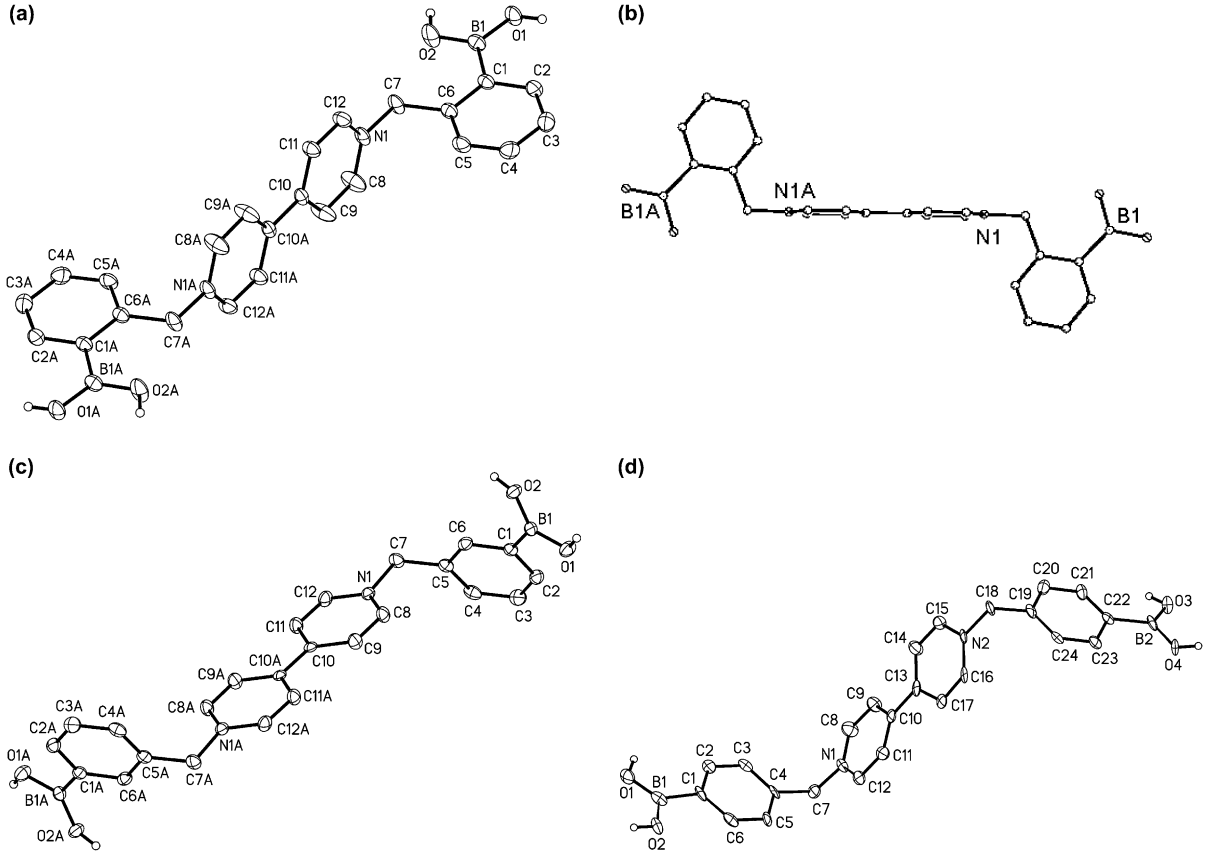

Figure 2. X-ray crystal structures of (a) *o*-BBV, (b) side view of *o*-BBV, (c) *m*-BBV, and (d) *p*-BBV. Thermal ellipsoids are drawn at the 50% probability level.

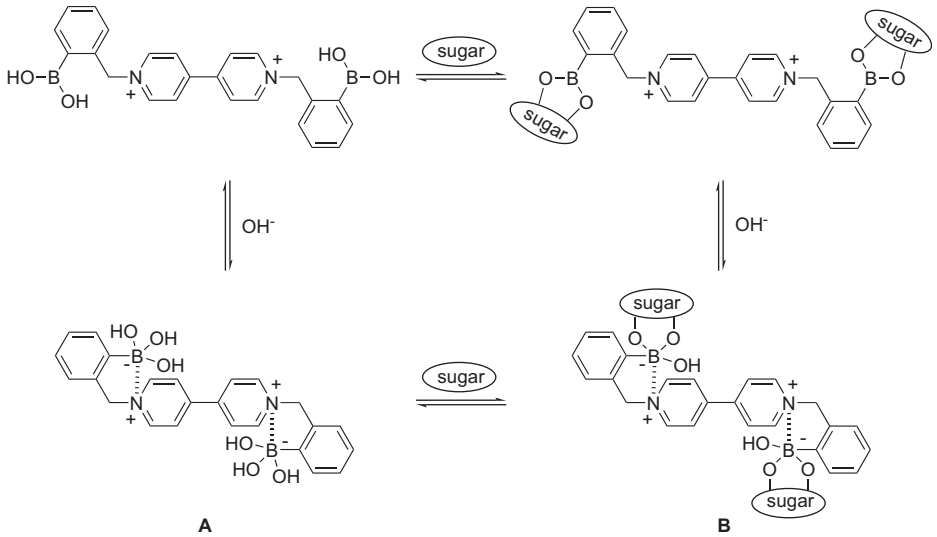

Scheme 3. The charge neutralization–stabilization mechanism of *o*-BBV. In structures **A** and **B**, dashed lines represent a charge interaction between the boronate and quaternary nitrogen.

occurrence of the proposed intramolecular electrostatic interaction for *o*-BBV.

2.2. Quenching of pyranine with the BBVs

For spectroscopic measurements to determine the relative quenching abilities of *o*-, *m*-, and *p*-BBV, a solution of pyranine (4×10^{-6} M in pH 7.4 phosphate buffer) was titrated with increasing amounts of the BBVs. The changes in the UV–vis absorbance spectra of pyranine upon addition of each of the viologens is shown in Figure 3. The bands at 404 and 454 nm represent the protonated and deprotonated forms of pyranine, respectively (due to the phenolic group). The addition of either *m*- or *p*-BBV to pyranine caused

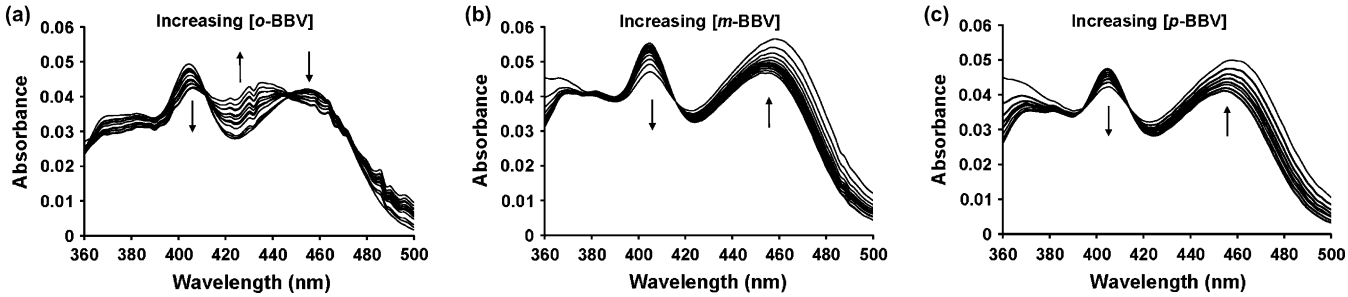

Figure 3. UV–vis absorbance spectra of pyranine (4×10^{-6} M in pH 7.4 phosphate buffer) with increasing concentrations of (a) *o*-BBV, (b) *m*-BBV, and (c) *p*-BBV.

a decrease in the 404 nm band and an increase in the 454 nm band. The addition of *o*-BBV, however, affected the absorbance of pyranine differently in that both the 404 and 454 nm bands decreased and a new band arose at 436 nm. These results indicate that *o*-BBV interacts with pyranine in a unique way.

The quenching efficiencies of each of the BBVs with pyranine were quantified using fluorescence measurements. The decrease in the fluorescence emission of pyranine (λ_{em}= 510 nm, λ_{ex}=460 nm) upon addition of *o*-BBV at pH 7.4 is demonstrated in Figure 4. Fluorescence quenching studies

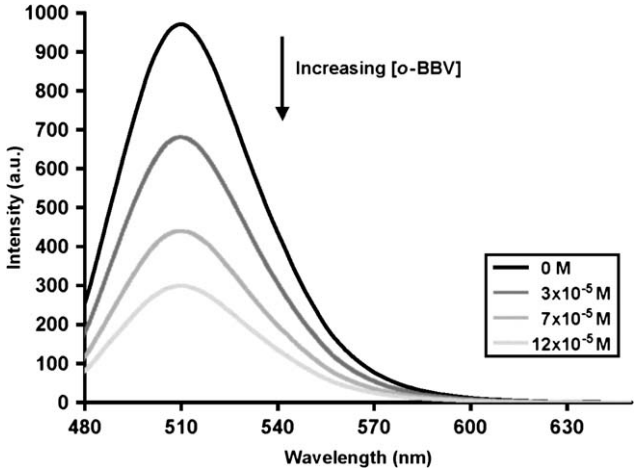

Figure 4. Fluorescence emission spectra of pyranine (4×10^{-6} M in pH 7.4 phosphate buffer, λ_{ex}=460 nm and λ_{em}=510 nm) with increasing concentrations of *o*-BBV.

were carried out at pH 3, 7.4, and 10. Stern–Volmer plots, which give graphical representations of the fluorescence data, are shown in Figure 5. From these plots, the static and dynamic quenching constants for BV and each of the BBVs were calculated using Eq. 1 (see Section 4), and are summarized in Table 1.

At pH 7.4 and 3, the BBVs are quite effective quenchers, giving static quenching constants around K_s~8000 M^{-1}. At pH 10 however, where the boronic acids are sp^3 hybridized and therefore anionic, the degree of quenching observed for all of the BBVs is greatly diminished (K_s~1500 M^{-1}) compared to that at pH 3 and 7.4. This is because formation of anionic boronates at pH 10 causes the BBVs to become zwitterionic, and a loss in electrostatic affinity for the anionic dye pyranine results. Conversely, for the non-boronic acid-containing compound, BV, the quenching constants were greatest at pH 10. This type of behavior for non-boronic acid-containing viologens has been observed in previous studies,[21] and is expected since Coulombic attraction in the ground-state is maximized at high pH.[18g]

When comparing each of the quenchers within a given pH range, we observe that at neutral or low pH values, the quenching efficiencies of *o*-, *m*-, and *p*-BBV are of similar magnitudes. But, at pH 10, the quenching efficiency of *o*-BBV is less than half that of *m*- and *p*-BBV. This dissimilarity of *o*-BBV from *m*- and *p*-BBV at high pH can be explained by evoking the charge neutralization–stabilization mechanism previously described (Scheme 3). For *o*-BBV at high pH, an intramolecular charge interaction can occur between the anionic boron and the quaternary nitrogen

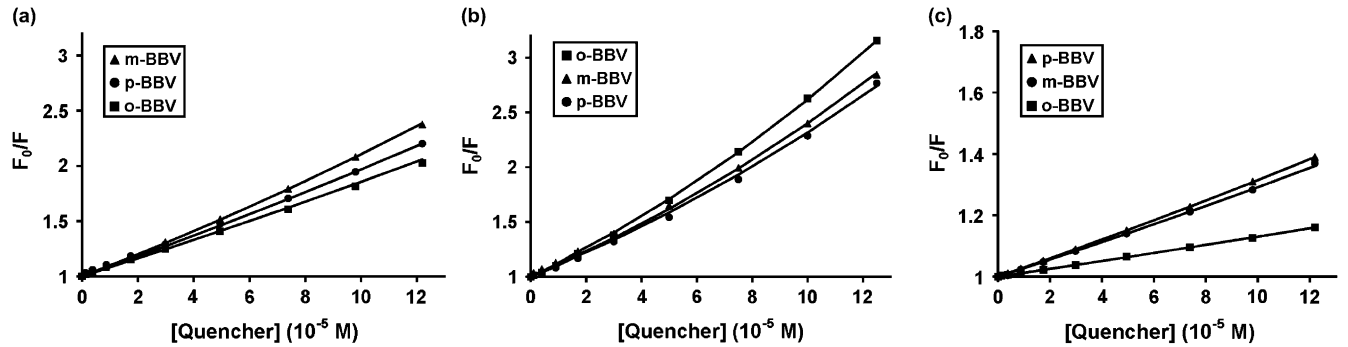

Figure 5. Stern–Volmer plots of pyranine (4×10^{-6} M) with increasing concentrations of *o*-BBV (■), *m*-BBV (▲), and *p*-BBV (●) at (a) pH 3, (b) pH 7.4, and (c) pH 10. For pH 3, λ_{ex}=416 nm and λ_{em}=510 nm. For pH 7.4 and 10, λ_{ex}=460 nm and λ_{em}=510 nm.

Table 1. Static (K_s) and dynamic (V) quenching constants for BV, *o*-BBV, *m*-BBV, and *p*-BBV with pyranine (4×10^{-6} M) in buffered 0.1 ionic strength solutions at different pH values

	pH 3		pH 7.4		pH 10	
	K_s (M^{-1})	V (M^{-1})	K_s (M^{-1})	V (M^{-1})	K_s (M^{-1})	V (M^{-1})
o-BBV	7300±100	750±100	8900±200	2900±200	670±80	570±60
m-BBV	8200±100	1400±150	7800±100	3100±100	2000±100	750±100
p-BBV	8000±100	890±180	7600±250	2700±150	2100±100	800±100
BV	10,000±200	1100±200	14,000±200	2500±200	25,000±200	3000±200

(structure A, Scheme 3).[†] This interaction allows for more effective neutralization of the cationic viologen, which results in less effective quenching of pyranine with *o*-BBV at pH 10 relative to *m*- and *p*-BBV.

2.3. pK_a Determination methods

It has been shown that the pK_a values for arylboronic acids are dependent upon the substitution pattern and nature of the substituents on the aromatic ring.[27–35] We therefore expected to see a lowered pK_a for the BBVs relative to phenylboronic acid (pK_a=8.8)[36] due to the methylpyridinuim substituent. Several different methods have been used to measure boronic acid pK_a values, such as UV–vis spectroscopy,[22,23,27–29] fluorescence spectroscopy,[12,30,31,37] cyclic voltammetry,[38] ^{11}B NMR,[21,35,39] and potentiometric titration.[16,39b,40] Determinations of pK_a values using UV–vis spectroscopy are carried out by monitoring the change in absorbance of the arylboronic acid upon increasing pH, which occurs as a result of a differential molar absorbtivity between sp^2 boronic acid and the sp^3 boronate. For our benzyl viologen-based boronic acids, however, the UV–vis titration method did not produce clean pH profiles. The use of fluorescence spectroscopy to measure boronic acid pK_a values is usually carried out by monitoring the change in fluorescence emission of a fluorophore-containing boronic acid upon increasing pH, which often occurs due to a photo-induced electron transfer (PET) mechanism brought about upon conversion to the sp^3 boronate. But, since the benzyl viologen-based boronic acids used in this study do not fluoresce, only indirect methods of measuring their apparent pK_a values via fluorescence are possible. Such analyses, however, are beyond the scope of this study.

For most systems, the use of ^{11}B NMR spectroscopy to determine boronic acid pK_a values is a reliable technique. We were able to generate pH profiles for the BBVs using ^{11}B NMR by observing the chemical shift dependence of the boron moiety on pH (Fig. 6). At low pH values, the boronic acids exist in their neutral sp^2 form and display a chemical shift of ~30 ppm. Increasing addition of base resulted in conversion to the anionic sp^3 form, causing a gradual upfield shift to lower parts per million values (Fig. 7). The apparent pK_a values for *m*- and *p*-BBV obtained by this method correlated fairly well with values previously reported for similar compounds.[‡] However, the value obtained for *o*-BBV (pK_a=8.8) seemed unreasonably high. We suspect that the mechanism proposed in Scheme 3 is

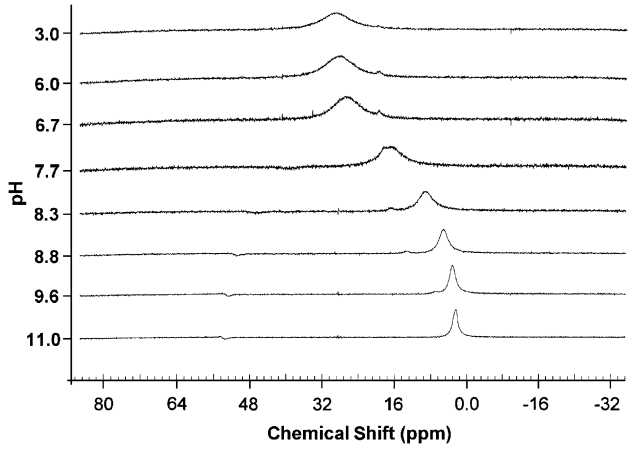

Figure 7. Changes in ^{11}B NMR spectrum of *m*-BBV with increasing pH (30 mM *m*-BBV in 0.15 M KCl titrated with 3 M KOH).

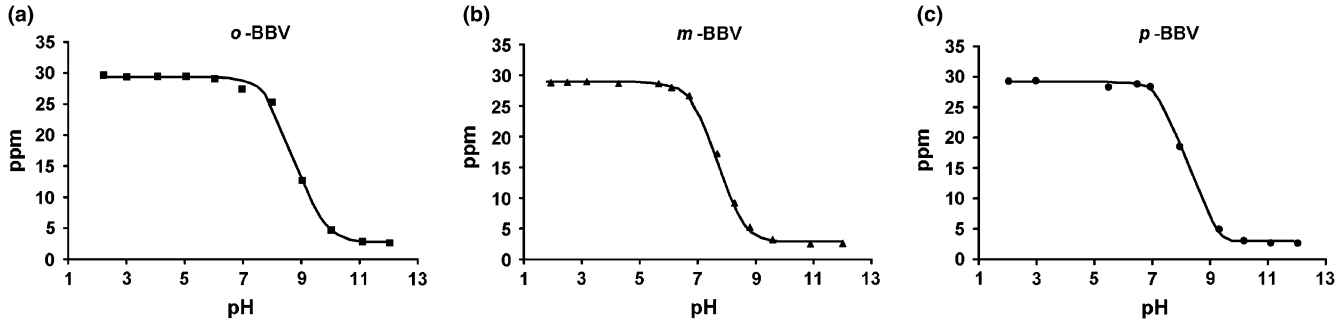

Figure 6. Determination of pK_a by ^{11}B NMR (30 mM BBV in 0.15 M KCl titrated with 3 M KOH). The pH profiles of (a) *o*-BBV, (b) *m*-BBV, and (c) *p*-BBV plotted as chemical shift versus pH.

[†] Structure **A** was optimized at the semi-empirical AM1 level using Spartan. The molecular modeling data indicate B–N interaction (see Supplementary data).

[‡] See Figure 9 and references listed in Table 2.

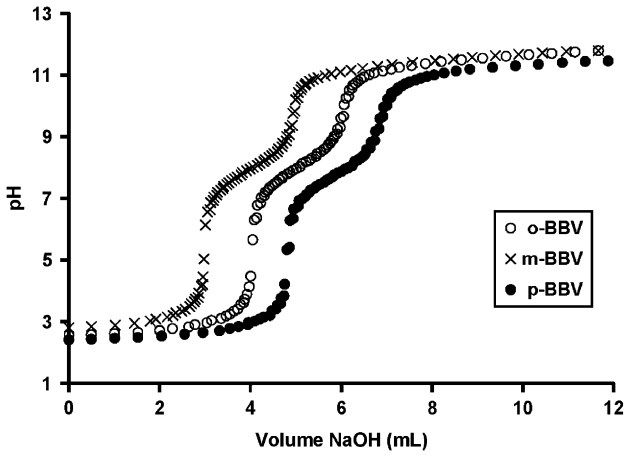

Figure 8. pH profile of *o*-BBV (○), *m*-BBV (×), and *p*-BBV (●) generated via potentiometric titration (4 mM BBV and HCl titrated with 0.1 M NaOH in 0.15 M NaCl; the pH at the halfway point equals the pK_a).

responsible for this misleading result, since neutralization of the negative charge on sp^3 boron by the quaternary nitrogen can cause higher chemical shift values than normal for the boronate by minimizing shielding effects.

Of the possible pK_a determination methods, we found potentiometric titration to be most suitable for the particular boronic acids under investigation, specifically *o*-BBV. Figure 8 shows the pH profiles for *o*-, *m*-, and *p*-BBV generated by potentiometric titration. Table 2 summarizes the pK_a results for both methods employed and, for comparison, lists pK_a values found in the literature for compounds containing a similar boronic acid-substituted benzyl pyridinium motif (Fig. 9). In contrast to the results obtained by ^{11}B NMR, the pK_a of *o*-BBV determined by potentiometric titration (8.0) was very similar to those determined for *m*- and *p*-BBV (7.9 and 7.7, respectively). These values were found to correlate quite well with pK_as reported in the literature for structurally similar boronic acids.

Table 2. Comparison of apparent pK_a values for the BBVs determined via ^{11}B NMR and potentiometric titration with literature values reported for structurally similar (Fig. 9) compounds

	^{11}B NMR	Potentiometric titration	Literature values[a]		
			Ref. 23[b]	Ref. 22[b]	Ref. 16[c]
o-BBV	8.8	8.0	7.9 (3*ortho*)	6.70 (4*ortho*)	7.73 (5*ortho*)
m-BBV	7.8	7.9	7.7 (3*meta*)	7.75 (4*meta*)	
p-BBV	8.1	7.7	7.9 (3*para*)	7.80 (4*para*)	7.92 (5*para*)

[a] See Figure 9.
[b] Determined by UV–vis absorbance spectroscopy.
[c] Determined by potentiometric titration.

2.4. Saccharide sensing

As described in Scheme 2, signal modulation in response to varying glucose concentrations occurs when glucose is added to a solution of pyranine that has been quenched by a BBV. When the glucoboronic ester forms, the Lewis acidity of boron is increased, facilitating 'ate' complex formation, and the BBV becomes partially zwitterionic at pH 7.4. This change in hybridization of the boron moiety from sp^2 to sp^3 upon glucose addition can be seen by ^{11}B NMR (Fig. 10), where the signal for trigonal boron at ~30 ppm decreases and a new signal at ~8 ppm for the tetrahedral glucoboronate ester arises.

This change in charge of the BBV decreases its ability to effectively quench the fluorescence of pyranine via static quenching. Since the structure of *o*-BBV is such that a through-space neutralization of the quaternary nitrogen by the anionic glucoboronate is feasible (structure B, Scheme 3), we rationalized that it should be the least effective quencher in the presence of glucose relative to *m*- or *p*-BBV. Accordingly, a comparison of the Stern–Volmer quenching constants determined for *o*-, *m*-, and *p*-BBV in the presence of 20 mM glucose revealed this to be the case. Figure 11 shows a Stern–Volmer plot of pyranine with *o*- and *m*-BBV in the absence and presence of glucose, where it can be seen that the quenching ability of *o*-BBV decreases most dramatically in the presence of glucose. Table 3 summarizes these data and gives the difference in quenching constants (ΔK_s and ΔV) with and without glucose. The presence of glucose did not affect the quenching ability of the control compound, BV.

According to our proposed glucose-sensing mechanism (Scheme 2), the fluorescence increase obtained when glucose is added to the system results from a decrease in the quenching efficiency of the glucoboronate ester compared to that of the free boronic acid. Therefore, since *o*-BBV is the weakest quencher in the presence of glucose (Table 3), we expected the *o*-BBV/pyranine complex to display the

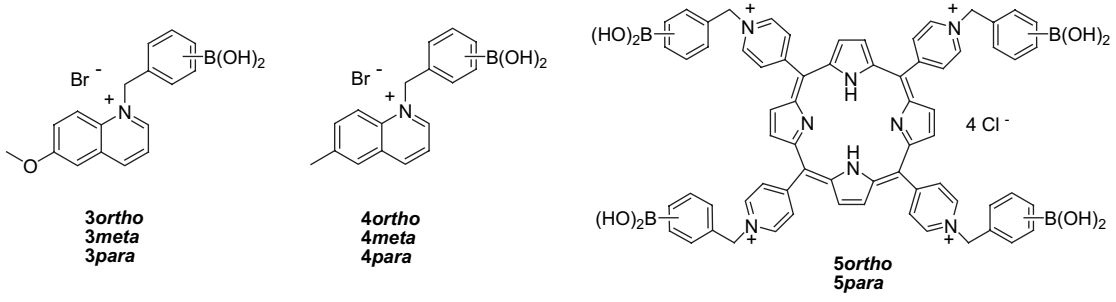

Figure 9. Structures of compounds **3**,[23] **4**,[22] and **5**[16] containing a boronic acid-substituted benzyl pyridinium motif for which pK_a values have been previously reported (Table 2).

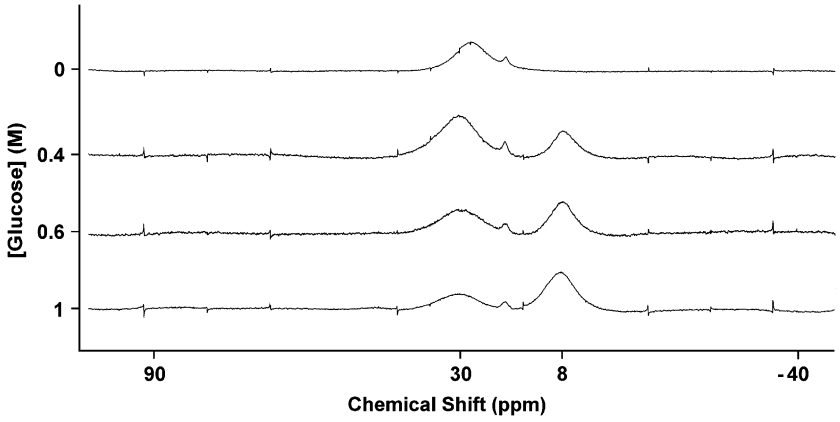

Figure 10. Changes in ^{11}B NMR spectrum of *m*-BBV (30 mM in pH 7.4 phosphate buffer) with increasing concentrations of glucose. High concentrations of glucose were used in order to achieve [quencher]/[glucose] ratios similar to those used in fluorescence studies. The small peak at 19 ppm is due to boric acid.

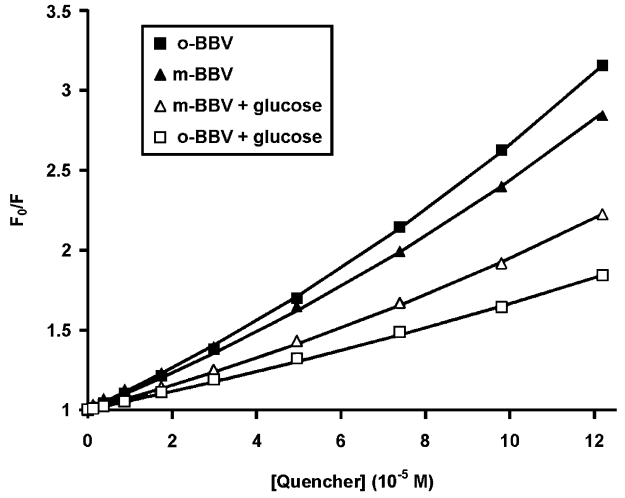

Figure 11. Stern–Volmer plot for the quenching of pyranine (4×10^{-6} M in pH 7.4 phosphate buffer, λ_{ex}=460 nm and λ_{em}=510 nm) with *m*-BBV (▲), *m*-BBV in the presence of 20 mM glucose (△), *o*-BBV (■), and *o*-BBV in the presence of 20 mM glucose (□).

largest fluorescence modulation upon glucose addition relative to *m*- and *p*-BBV/pyranine. For glucose-sensing experiments, BBV is added to a solution of pyranine, and the quenched fluorescence intensity is recorded. Increasing concentrations of glucose are then added to the BBV/pyranine complex and enhanced fluorescence intensities are observed (Fig. 12a). Figure 12b shows the degree of fluorescence enhancement obtained for each of the quencher/dye complexes plotted as a function of glucose concentration, where it can be seen that *o*-BBV exhibits the highest fluorescence modulation out of the three receptors. Importantly, all the BBVs displayed considerable fluorescence enhancements

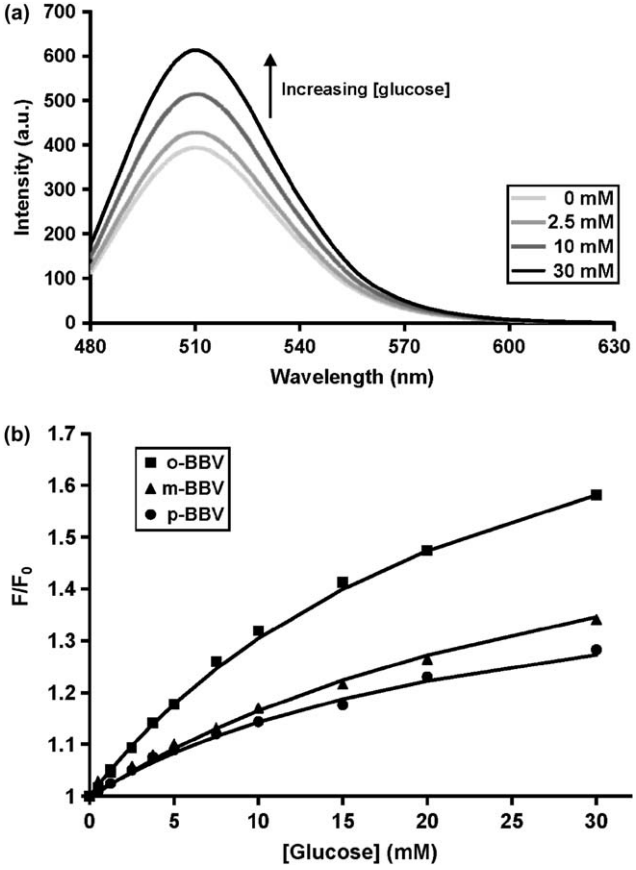

Figure 12. Glucose sensing of BBVs (1.2×10^{-4} M) with pyranine (4×10^{-6} M in pH 7.4 phosphate buffer, λ_{ex}=460 nm and λ_{em}=510 nm). (a) Change in fluorescence spectrum of pyranine in the presence of *o*-BBV upon addition of glucose. (b) Binding isotherms: fluorescence increase of pyranine in the presence of *o*-BBV (■), *m*-BBV (▲), and *p*-BBV (●) as a function of glucose concentration.

Table 3. Static (K_s) and dynamic (V) quenching constants of *o*-BBV, *m*-BBV, *p*-BBV, and BV with pyranine (4×10^{-6} M in pH 7.4 phosphate buffer, λ_{ex}=460 nm and λ_{em}=510 nm) in the absence and presence of glucose (20 mM)

	Absence of glucose		Presence of 20 mM glucose		Change	
	K_s (M^{-1})	V (M^{-1})	K_s (M^{-1})	V (M^{-1})	ΔK_s	ΔV
o-BBV	8900±200	2900±200	3000±100	2400±100	5900	500
m-BBV	7800±100	3100±100	4000±100	3300±100	3800	200
p-BBV	7600±250	2700±150	3600±100	2900±100	4000	200
BV	14,000±200	2500±200	14,000±200	2100±200	0	400

in response to glucose concentrations within the clinically relevant range of 45–360 mg dL^{-1} (2.5–20 mM).

The calculated apparent binding constants (K_b) listed in Table 4 show that *o*-BBV also has the largest binding constant, which is consistent with an enhanced stabilization of the glucoboronate ester. Previously, BV was shown to be unresponsive to glucose in this system.[13]

The BBVs were also tested for their ability to bind other monosaccharides such as fructose and galactose (Fig. 13). The saccharide selectivity for all of the quencher/receptors was found to be of the order fructose>galactose>glucose. This binding order is parallel to that observed for monoboronic acids, indicating that cooperative binding is not taking place.[6,9] Table 4 lists the calculated apparent binding constants (K_b) for each of the BBVs with the different monosaccharides.

Finally, the pK_a values for *o*-, *m*-, and *p*-BBV in the presence of glucose were obtained by potentiometric titration (Fig. 14). *o*-BBV displayed the largest drop in pK_a in the presence of glucose (ΔpK_a) relative to *m*- or *p*-BBV (Table 5), again indicating an enhanced stabilization of the boronate ester. The results further substantiate that the proposed charge neutralization–stabilization mechanism is operative for *o*-BBV.

Table 4. Apparent saccharide binding constants (K_b) determined for the BBVs (1.2×10^{-4} M) with pyranine (4×10^{-6} M in phosphate buffer, λ_{ex}=460 nm and λ_{em}=510 nm)

	Glucose	Galactose	Fructose
	K_b (M^{-1})	K_b (M^{-1})	K_b (M^{-1})
o-BBV	45±5	150±5	2000±100
m-BBV	30±3	85±5	1200±100
p-BBV	33±3	70±5	800±50

Table 5. pK_a values, determined by potentiometric titration, for the BBVs (4 mM) in the absence and presence of 0.3 M glucose

	pK_a without glucose	pK_a with 0.3 M glucose	ΔpK_a
o-BBV	8.0	6.3	1.7
m-BBV	7.9	6.5	1.4
p-BBV	7.7	6.5	1.2

3. Conclusions

For the glucose-sensing ensemble comprising a boronic acid-substituted benzyl viologen and the anionic dye pyranine, a systematic investigation of the effect of boronic acid-positioning on both the quenching and glucose-sensing mechanisms was performed. Under conditions where the anionic boronate is formed, such as at pH 10 and in the presence of glucose at pH 7.4, the benzyl viologen that contains *ortho*-substituted boronic acids, *o*-BBV, stood out from the other two (*m*- and *p*-BBV) presumably as a result of the intramolecular electrostatic interaction between the anionic boronate and the quaternary nitrogen. Apparent pK_a data obtained from ^{11}B NMR studies and potentiometric titration helped confirm the occurrence of this mechanism in *o*-BBV. From the standpoint of sensor design, in this type of two-component system, having the boron in a position where the negative charge resulting from sugar complexation

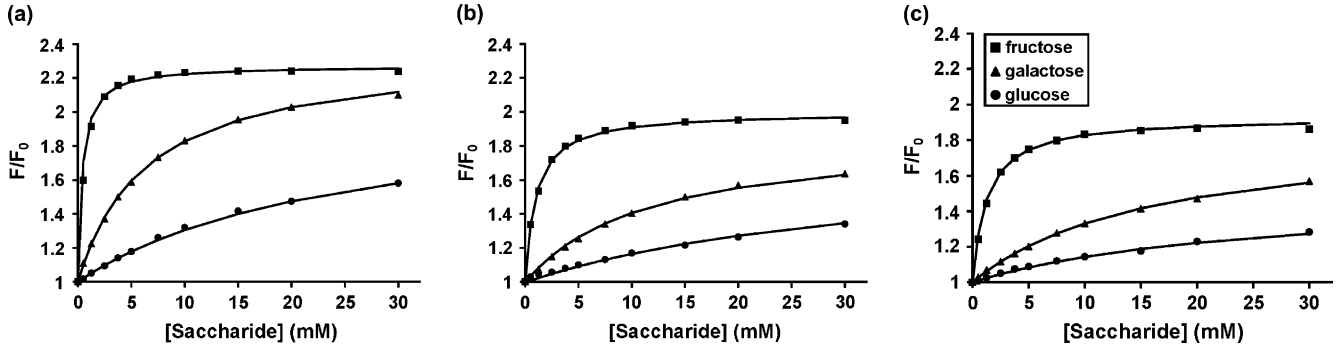

Figure 13. Fluorescence increase of pyranine (4×10^{-6} M in phosphate buffer, λ_{ex}=460 nm and λ_{em}=510 nm) in the presence of (a) *o*-BBV, (b) *m*-BBV, and (c) *p*-BBV (1.2×10^{-4} M) upon addition of different monosaccharides.

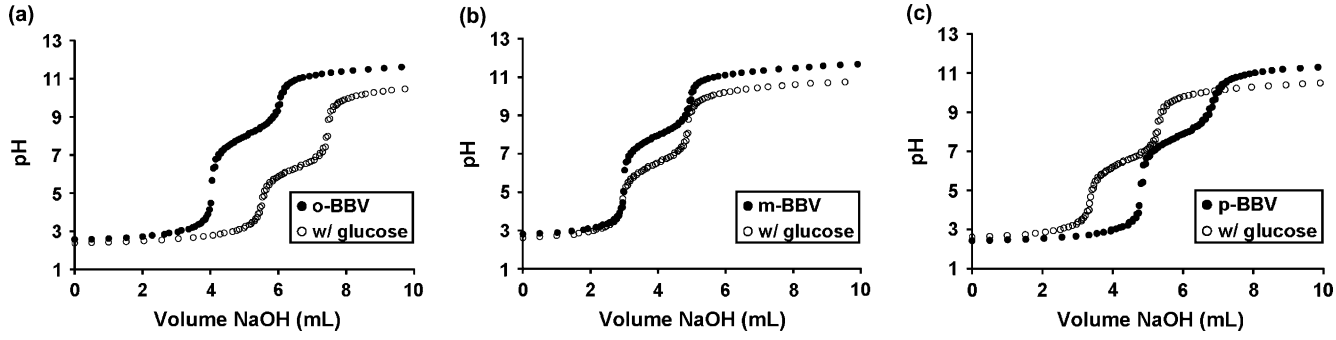

Figure 14. pH profile of (a) *o*-BBV, (b) *m*-BBV, and (c) *p*-BBV in the absence (●) and presence (○) of 0.3 M glucose generated via potentiometric titration (4 mM BBV titrated with 0.1 M NaOH in 0.15 M NaCl; the pH at the halfway point equals the pK_a).

can more effectively neutralize the positive charge of the viologen is most desirable.

4. Experimental

4.1. Synthesis

The syntheses of *o*-BBV[13] and *m*-BBV[20] have been previously reported.

4.1.1. General. Reactions were performed using standard syringe techniques, and carried out in an oven-dried glassware under an argon atmosphere. Dimethylformamide (DMF) was dried over CaH_2 prior to use. 4-Bromomethyl phenylboronic acid was purchased from Lancaster and used as received. Benzyl bromide and 4,4′-dipyridyl were purchased from Aldrich and used as received. ^{1}H NMR spectra were recorded on a Varian spectrometer at 500 MHz and are reported in parts per million with respect to TMS (δ=0). Proton decoupled ^{13}C NMR spectra were recorded on a Varian at 125 MHz and are reported in parts per million.[§] ^{11}B NMR spectra were recorded on a Bruker at 80.25 MHz and are reported in parts per million with respect to $BF_3\cdot OEt_2$ (δ=0). High-resolution mass measurements were obtained on a bench-top Mariner ESITOF mass spectrometer.

4.1.2. *N*,*N*′-4,4′-Bis(benzyl-4-boronic acid)-bipyridinium dibromide (*p*-BBV). To a solution of 4-(bromomethyl)-phenylboronic acid (1.74 g, 8.1 mmol) in DMF (15 mL) was added 4,4′-dipyridyl (0.5 g, 3.2 mmol), and the reaction mixture was stirred at 55 °C for 48 h. The orange precipitate was collected by centrifugation, washed with DMF, then acetone, and dried under a stream of argon to yield *p*-BBV (1.3 g, 69% yield). ^{1}H NMR (D_2O, 500 MHz) δ 6.09 (s, 4H), 7.67 (d, J=8.0 Hz, 4H), 7.98 (d, J=7.5 Hz, 4H), 8.68 (d, J=7.0 Hz, 4H), 9.30 (d, J=7.0 Hz, 4H); ^{13}C NMR (D_2O, 125 MHz) δ 66.1, 128.6, 130.0, 136.08, 136.2, 147.05, 147.12, 151.8; ^{11}B NMR (80 MHz, D_2O) δ 28.9. HRMS–ESI *m*/*z* calcd for $C_{24}H_{23}B_2N_2O_4$ $[M-H]^+$: 425.18301, found 425.18385.

4.1.3. *N*,*N*′-4,4′-Bis(benzyl)-bipyridinium dibromide (BV). To a solution of benzyl bromide (0.45 mL, 3.75 mmol) in DMF (5 mL) was added 4,4′-dipyridyl (0.23 g, 1.5 mmol), and the reaction mixture was stirred at 70 °C for 16 h. The yellow precipitate was collected by centrifugation, washed with acetone, and dried under a stream of argon to yield pure BV (0.67 g, 90% yield). Spectroscopic data were in accord with the literature values.[41]

4.2. X-ray structure determinations

X-ray single crystal diffraction experiments were carried out on a Bruker SMART 1000 for [*o*-BBV]Br_2 and [*m*-BBV]$Br_2\cdot H_2O$ and a Bruker SMART Apex for [*p*-BBV]$Br_2\cdot 5H_2O$ with the use of Mo Kα radiation (λ=0.71073 Å). The data for *o*-BBV were collected at 166(2) K due to cracking of the crystals at temperatures lower than this. Data for *m*-BBV and *p*-BBV were collected at 90(2) K. Solution and refinement software were SAINT for data reduction, SHELXS97 for solution, and SHELXL97 for refinement. In the structures of [*o*-BBV]Br_2 and [*m*-BBV]$Br_2\cdot H_2O$ the cations reside on centers of symmetry, and this requires the bipyridine planes to be coplanar. In the structure of [*p*-BBV]$Br_2\cdot 5H_2O$, there are two independent molecules in the asymmetric unit, and the normals to the bipyridine planes subtend dihedral angles of 16.5° and 23.9° for the two different molecules. Disordered water molecules of crystallization caused the *R* value to be somewhat elevated for this latter structure. Crystallographic data for the structures in this paper have been deposited with the Cambridge Crytallographic Data Centre as supplementary publication numbers CCDC 298628-298630. Copies of the data can be obtained, free of charge, on application to CCDC, 12 Union Road, Cambridge CB2 1EZ, UK [fax: +44 1223 336033 or e-mail: deposit@ccdc.cam.ac.uk].

4.2.1. [*o*-BBV]Br_2. $C_{24}H_{24}B_2Br_2N_2O_4$, M=585.89, monoclinic, a=9.0541(7) Å, b=9.6817(8) Å, c=14.3909(12) Å, β=107.574(2)°, V=1202.62(17) Å^3, space group $P2_1/c$, Z=2, T=166(2) K, D_{calcd}=1.618 mg m^{-3}, μ(Mo Kα)=3.405 mm^{-1}, 13,306 reflections measured, 2771 unique (R_{int}=0.039) used in all calculations. The final *wR*2 was 0.0779 (all data) and $R_1(2165I>2\sigma(I))$=0.0306. Residual electron density was 0.444 and −0.346 eÅ^{-3}.

4.2.2. [*m*-BBV]$Br_2\cdot H_2O$. $C_{24}H_{26}B_2Br_2N_2O_5$, M=603.91, monoclinic, a=14.3954(11) Å, b=14.0371(9) Å, c=12.7590(9)Å, β=104.299(2)°, V=2498.3(3) Å^3, space group $P2_1/c$, Z=4, T=90(2) K, D_{calcd}=1.606 mg m^{-3}, μ(Mo Kα)=3.283 mm^{-1}, 25,461 reflections measured, 5733 unique (R_{int}=0.045) used in all calculations. The final *wR*2 was 0.0717 (all data) and $R_1(4372I>2\sigma(I))$=0.0293. Residual electron density was 0.490 and −0.329 eÅ^{-3}.

4.2.3. [*p*-BBV]$Br_2\cdot 5H_2O$. $C_{24}H_{34}B_2Br_2N_2O_9$, M=675.97, monoclinic, a=16.932(5) Å, b=28.674(8) Å, c=12.118(3) Å, β=103.963(5)°, V=5710(3) Å^3, space group $P2_1/c$, Z=8, T=90(2) K, D_{calcd}=1.573 mg m^{-3}, μ(Mo Kα)=2.892 mm^{-1}, 53,403 reflections measured, 10,494 unique (R_{int}=0.151) used in all calculations. The final *wR*2 was 0.2178 (all data) and $R_1(6197I>2\sigma(I))$=0.0827. Residual electron density was 1.784 and −1.363 eÅ^{-3}.

4.3. Fluorescence emission and UV–vis absorption measurements

4.3.1. General. 8-Hydroxypyrene-1,3,6-trisulfonic acid, trisodium salt (pyranine), D-glucose, D-glactose, and D-fructose were purchased from Aldrich. All solutions were prepared with water that was purified via a Barnstead NANOpure system (17.7 MΩ/cm). Buffers (0.1 ionic strength) were freshly prepared before use (pH 3: KH_2PO_4, H_3PO_4; pH 7.4: KH_2PO_4, Na_2HPO_4; pH 10: Na_2CO_3, $NaHCO_3$). pH measurements were taken on a Denver Instrument UB-10 pH/mV meter and calibrated with standard buffer solutions (pH 4, 7, and 10 from Fisher). Absorption spectra were taken on a Hewlett Packard 8452A Diode Array Spectrophotometer. Fluorescence spectra were taken on a Perkin–Elmer LS50-B luminescence spectrometer, and were carried out at 25 °C. Standard quartz fluorescence cuvettes were used in all studies. Pyranine was excited at two different wavelengths depending on the pH. For samples run at pH 3, the

[§] Due to relaxed ^{13}C–^{11}B spin–spin coupling, signals for carbons directly attached to boron are not observed.

excitation was 416 nm; for samples run at pH 7.4 and 10, the excitation was 460 nm. The emission was collected from 470 to 650 nm. Pyranine is known to undergo an excited state proton transfer reaction in bulk water where water acts as the proton acceptor.[42] Thus, the emission collected at pH 3, 7.4, or 10 corresponds to the emission of the deprotonated form of pyranine. For fluorescence titration experiments, the added volume did not exceed 3% of the total volume and the absorbance for all fluorescence measurements was below 0.1.[43] All experiments were carried out in triplicate, and the errors in the reported binding constants are based on the standard deviation of three independent determinations. All data were analyzed using the Solver (nonlinear least-squares curve fitting) in Microsoft Excel.

4.3.2. Absorbance measurements. Measurements were done in situ by taking the absorbance spectra of pyranine with each of the quenchers. The emission of pyranine (2 mL of 4×10^{-6} M in buffer) was first obtained, then aliquots of quencher (0.5–10 μL aliquots of 5 mM in buffer) were added, the solution was shaken for 30 s, and the absorbance was measured after each quencher addition.

4.3.3. Fluorescence measurements for quenching studies. Fluorescence measurements were done in situ by taking the emission spectrum of pyranine at a series of quencher concentrations. The emission spectrum of pyranine (2 mL of 4×10^{-6} M in buffer) was first obtained, quencher was added (0.5–10 μL aliquots of 5 mM in buffer), the solution was shaken for 30 s, and the new emission was measured after each quencher addition. For quenching studies carried out in the presence of glucose, the emission spectrum of pyranine (2 mL of 4×10^{-6} M in buffer) was first obtained, glucose was added (40 μL of 1.0 M in buffer), the emission measured, then quencher was added (0.5–10 μL aliquots of 5 mM in buffer), the solution was shaken for 30 s, and the new emission was measured after each quencher addition.

Data analysis: Fluorescence intensity was taken as the area under the curve between 470 and 650 nm for all studies. Stern–Volmer quenching constants were calculated by fitting the data with Eq. 1:

$$F_0/F = (1 + K_s[Q])e^{V[Q]} \quad (1)$$

where F_0 is the initial fluorescence intensity, F is the fluorescence intensity after the addition of quencher, V is the dynamic quenching constant, K_s is the static quenching constant, and $[Q]$ is the quencher concentration.[18a,44]

4.3.4. Fluorescence measurements for saccharide sensing studies. The emission spectrum of pyranine (2 mL of 4×10^{-6} M in buffer) was taken, quencher was added (50 μL of 5 mM in buffer) to obtain a quencher/pyranine ratio of 31:1, the emission measured, then sugar solution was added (0.5–10 μL aliquots of 1 M in buffer), the solution was shaken for 30 s, and the new emission was measured after each addition of sugar.

Data analysis: Fluorescence intensity was taken as the area under the curve between 470 and 650 nm for all studies. Apparent sugar binding constants were calculated by fitting the data with Eq. 2:

$$F/F_0 = (F_0 + F_{max}K_b[S])/(1 + K_b[S]) \quad (2)$$

where F_0 is the fluorescence intensity of the quenched dye, F is the fluorescence intensity after the addition of sugar, F_{max} is the intensity at which the fluorescence increase reaches its maximum, K_b is the apparent binding constant, and $[S]$ is the concentration of sugar (glucose, fructose, or galactose).[37b]

4.4. ^{11}B NMR titrations

A 2 mL solution quencher (0.03 M) containing 0.15 M KCl was lowered to pH 2 by the addition of 3 M HCl. A 5-mm quartz NMR tube (Norell) was charged with 0.75 mL of this solution and a spectrum was recorded. The contents of the tube were added to the original 2 mL solution, and the pH was raised in increments of 0.5–1 pH unit by adding 3 M KOH. The ^{11}B NMR spectrum was taken after each pH adjustment until pH 12. The pK_as were calculated using Eq. 3:

$$PPM_{calc} = \left(PPM_{min} + PPM_{max}10^{pK_a}\left[H^+\right]\right)/\left(1 + 10^{pK_a}\left[H^+\right]\right) \quad (3)$$

where PPM_{calc} is the calculated chemical shift in parts per million, PPM_{min} is the initial chemical shift, PPM_{max} is the final chemical shift, pK_a is the acidity constant, and $[H^+]$ is the hydrogen ion concentration.[37b]

4.5. Potentiometric titrations

Potentiometric studies were conducted with a KEM AT-500N automatic titrator equipped with a combined pH glass electrode (Ag/AgCl reference electrode) containing 3.3 M KCl internal filling solution. Measurements were taken at 25 °C. About 100 data points were collected for each titration and imported into Excel using the AT-Win software package. Solutions of boronic acid (4 mM in deionized water) were adjusted to pH ~2 with a drop of concd HCl, then titrated with 0.1 M NaOH in 0.15 M NaCl. Two endpoints were detected (one for HCl and one for the boronic acid). For the weak acid–strong base titration curve of the boronic acid, the pK_a was determined from the halfway point in the titration.

Acknowledgements

We thank the BioSTAR Project and the Industry–University Cooperative Research Program (grant bio04-10458) with GluMetrics, Inc. for their financial support.

Supplementary data

Molecular modelling data for structure A (Scheme 3). ^{1}H and ^{13}C NMR spectra for *p*-BBV. Supplementary data associated with this article can be found in the online version, at doi:10.1016/j.tet.2006.04.047.

References and notes

1. For recent reviews see: (a) Wang, W.; Gao, X.; Wang, B. *Curr. Org. Chem.* **2002**, *6*, 1285–1317; (b) James, T. D.; Shinkai, S.

Top. Curr. Chem. **2002**, *218*, 159–200; (c) Striegler, S. *Curr. Org. Chem.* **2003**, *7*, 81–102; (d) Cao, H.; Heagy, M. D. *J. Fluoresc.* **2004**, *14*, 569–584.
2. Heinemann, L.; Schmelzeisen-Redeker, G. *Diabetologia* **1998**, *41*, 848–854.
3. McNichols, R. J.; Cote, G. L. *J. Biomed. Opt.* **2000**, *5*, 5–16.
4. Khalil, O. S. *Clin. Chem.* **1999**, 165–177.
5. Koschinsky, T.; Heinemann, L. *Diabetes Metab. Res. Rev.* **2001**, 113–123.
6. Lorand, J. P.; Edwards, J. *J. Org. Chem.* **1959**, *24*, 769–774.
7. James, T. D.; Sandanayake, K. R. A. S.; Iguchi, R.; Shinkai, S. *J. Am. Chem. Soc.* **1995**, *117*, 8982–8987.
8. Norrild, J. C.; Sotofte, I. *J. Chem. Soc., Perkin Trans. 2* **2001**, 727–732.
9. Springsteen, G.; Wang, B. *Tetrahedron* **2002**, *58*, 5291–5300.
10. Rohovec, J.; Maschmeyer, T.; Aime, S.; Peters, J. A. *Chem.—Eur. J.* **2003**, *9*, 2193–2199.
11. For reviews see: (a) Pickup, J. C.; Hussain, F.; Evans, N. D.; Rolinski, O. J.; Birch, D. J. S. *Biosens. Bioelectron.* **2005**, *20*, 2555–2565; (b) Moschou, E. A.; Sharma, B. V.; Deo, S. K.; Daunert, S. *J. Fluoresc.* **2004**, *14*, 535–547; (c) Fang, H.; Kaur, G.; Wang, B. *J. Fluoresc.* **2004**, *14*, 481–489; (d) Kawanishi, T.; Romey, M. A.; Zhu, P. C.; Holody, M. Z.; Shinkai, S. *J. Fluoresc.* **2004**, *14*, 499–512; (e) Czarnik, A. W. *Fluorescent Chemosensors for Ion and Molecule Recognition*; American Chemical Society: Washington, DC, 1993.
12. Yoon, J.; Czarnik, A. W. *J. Am. Chem. Soc.* **1992**, *114*, 5874–5875.
13. Camara, J. N.; Suri, J. T.; Cappuccio, F. E.; Wessling, R. A.; Singaram, B. *Tetrahedron Lett.* **2002**, *43*, 1139–1141.
14. For two-component glucose sensing systems using an Alizarin Red-based competitive assay see: (a) Arimori, S.; Ward, C. J.; James, T. D. *Tetrahedron Lett.* **2002**, *43*, 303–305; (b) Springsteen, G.; Wang, B. *Chem. Commun.* **2001**, 1608–1609; (c) Ref. 9.
15. For a review of E. V. Anslyn's two-component system for sensing other analytes see: Wiskur, S. L.; Ait-Haddou, H.; Lavigne, J. J.; Anslyn, E. V. *Acc. Chem. Res.* **2001**, *34*, 963–972.
16. Arimori, S.; Murakami, H.; Takeuchi, M.; Shinkai, S. *J. Chem. Soc., Chem. Commun.* **1995**, 961–962.
17. DiCesare, N.; Pinto, M. R.; Schanze, K. S.; Lakowicz, J. R. *Langmuir* **2002**, *18*, 7785–7787.
18. For studies involving fluorescence quenching with viologens see: (a) de Borba, E. B.; Amaral, C. L. C.; Politi, M. J.; Villalobos, R.; Baptista, M. S. *Langmuir* **2000**, *16*, 5900–5907; (b) Nakashima, K.; Kido, N. *Photochem. Photobiol.* **1996**, *64*, 296–302; (c) Zhao, Z. G.; Shen, T.; Xu, H. J. *J. Photochem. Photobiol., A* **1990**, *52*, 47–53; (d) Chen, L. H.; McBranch, D. W.; Wang, H. L.; Helgeson, R.; Wudl, F.; Whitten, D. G. *Proc. Natl. Acad. Sci. U.S.A.* **1999**, *96*, 12287–12292; (e) Gaylord, B. S.; Wang, S. J.; Heeger, A. J.; Bazan, G. C. *J. Am. Chem. Soc.* **2001**, *123*, 6417–6418; (f) Wang, D. L.; Gong, X.; Heeger, P. S.; Rininsland, F.; Bazan, G. C.; Heeger, A. J. *Proc. Natl. Acad. Sci. U.S.A.* **2002**, *99*, 49–53; (g) Wang, D. L.; Wang, J.; Moses, D.; Bazan, G. C.; Heeger, A. J. *Langmuir* **2001**, *17*, 1262–1266; (h) Serpone, N. *Photoinduced Electron Transfer*; Fox, M. A., Chanon, M., Eds.; Elsevier: Amsterdam, 1988; Vol. D, p 47.
19. Cordes, D. B.; Miller, A.; Gamsey, S.; Sharrett, Z.; Thoniyot, P.; Wessling, R. A.; Singaram, B. *Org. Biomol. Chem.* **2005**, *3*, 1708–1713.
20. Cordes, D. B.; Gamsey, S.; Sharrett, Z.; Miller, A.; Thoniyot, P.; Wessling, R. A.; Singaram, B. *Langmuir* **2005**, *21*, 6540–6547.
21. Suri, J. T.; Cordes, D. B.; Cappuccio, F. E.; Wessling, R. A.; Singaram, B. *Langmuir* **2003**, *19*, 5145–5152.
22. Badugu, R.; Lakowicz, J. R.; Geddes, C. D. *Talanta* **2005**, *65*, 762–768.
23. Badugu, R.; Lakowicz, J. R.; Geddes, C. D. *Bioorg. Med. Chem.* **2005**, *13*, 113–119.
24. Arimori, S.; Takeuchi, M.; Shinkai, S. *Supramol. Sci.* **1998**, *5*, 1–8.
25. Arimori, S.; Takeuchi, M.; Shinkai, S. *J. Am. Chem. Soc.* **1996**, *118*, 245–246.
26. Takeuchi, M.; Koumoto, K.; Goto, M.; Shinkai, S. *Tetrahedron* **1996**, *52*, 12931–12940.
27. Yan, J.; Springsteen, G.; Deeter, S.; Wang, B. *Tetrahedron* **2004**, *60*, 11205–11209.
28. Mulla, H. R.; Agard, N. J.; Basu, A. *Bioorg. Med. Chem. Lett.* **2004**, *14*, 25–27.
29. Ni, W.; Fang, H.; Springsteen, G.; Wang, B. *J. Org. Chem.* **2004**, *69*, 1999–2007.
30. (a) DiCesare, N.; Lakowicz, J. R. *J. Phys. Chem. A* **2001**, *105*, 6834–6840; (b) DiCesare, N.; Lakowicz, J. R. *Tetrahedron Lett.* **2002**, *43*, 2615–2618.
31. Cao, H.; McGill, T.; Heagy, M. *J. Org. Chem.* **2004**, *69*, 2959–2966.
32. Matsumoto, A.; Ikeda, S.; Harada, A.; Kataoka, K. *Biomacromolecules* **2003**, *4*, 1410–1416.
33. Westmark, P. R.; Gardiner, S. J.; Smith, B. D. *J. Am. Chem. Soc.* **1996**, *118*, 11093–11100.
34. Das, S.; Alexeev, L.; Sharma, A. C.; Geib, S. J.; Asher, S. A. *Tetrahedron Lett.* **2003**, *44*, 7719–7722.
35. Singhal, R. P.; Ramamurthy, B.; Govindraj, N.; Sarwar, Y. *J. Chromatogr.* **1991**, *543*, 17–38.
36. (a) Nakatani, H.; Morita, T.; Hiromi, K. *Biochim. Biophys. Acta* **1978**, *525*, 423–428; (b) Juillard, J.; Geuge, N. *Comp. Rend. Acad. Sci. C* **1967**, *264*, 259–261; (c) Branch, G. E. K.; Yabroff, D. L.; Bettman, B. *J. Am. Chem. Soc.* **1934**, *56*, 937–941; (d) Soundararajan, S.; Badawi, M.; Kohlrust, C. M.; Hageman, J. H. *Anal. Biochem.* **1989**, *178*, 125–134.
37. (a) Luis, P. G.; Granda, M.; Badia, R.; Diaz-Garcia, M. E. *Analyst* **1998**, *123*, 155–158; (b) Cooper, C. R.; James, T. D. *J. Chem. Soc., Perkin Trans. 1* **2000**, 963–969; (c) Arimori, S.; Bosch, L. I.; Ward, C. J.; James, T. D. *Tetrahedron Lett.* **2001**, *42*, 4553–4555; (d) Wang, J.; Jin, S.; Wang, B. *Tetrahedron Lett.* **2005**, *46*, 7003–7006; (e) Wang, Z.; Zhang, D.; Zhu, D. *J. Org. Chem.* **2005**, *70*, 5729–5732.
38. (a) Moore, A. N. J.; Wayner, D. D. M. *Can. J. Chem.* **1999**, *77*, 681–686; (b) Takahashi, S.; Kashiwai, Y.; Hoshi, T.; Anzai, J. *Anal. Sci.* **2004**, *20*, 757–759; (c) Takahashi, S.; Anzai, J. *Langmuir* **2005**, *21*, 5102–5107.
39. (a) Nagai, Y.; Kobayashi, K.; Toi, H.; Aoyama, Y. *Bull. Chem. Soc. Jpn.* **1993**, *66*, 2965–2971; (b) Wiskur, S. L.; Lavigne, J. J.; Ait-Haddou, H.; Lynch, V.; Chiu, Y. H.; Canary, J. W.; Anslyn, E. V. *Org. Lett.* **2001**, *3*, 1311–1314; (c) Liu, X.-C.; Scouten, W. H. *J. Chromatogr. A* **1994**, *687*, 61–69.
40. (a) Bosch, L. I.; Fyles, T. M.; James, T. D. *Tetrahedron* **2004**, *60*, 11175–11190; (b) Johnson, B. J. B. *Biochemistry* **1981**, *20*, 6103–6108.
41. Kamogawa, H.; Suzuki, T. *Bull. Chem. Soc. Jpn.* **1987**, *60*, 794–796.
42. Huppert, D.; Gutman, M.; Kaufmann, K. J. *Adv. Chem. Phys.* **1981**, *47*, 643–679.
43. Credi, A.; Prodi, L. *Spectrochim. Acta, Part A* **1998**, *54*, 159–170.
44. Frank, I. M.; Vavilov, S. I. Z. *Phys. Chem. (Munich)* **1931**, *69*, 100–110.